Published in final edited form as:
Circulation. 2004 March 2; 109(8): 1016–1021. doi:10.1161/01.CIR.0000116767.95046.C2.

Magnetic Resonance Imaging Identifies the Fibrous Cap in Atherosclerotic Abdominal Aortic Aneurysm

Christopher M. Kramer, MD, **Lisa A. Cerilli, MD**, **Klaus Hagspiel, MD**, **Joseph M. DiMaria, BA**, **Frederick H. Epstein, PhD**, and **John A. Kern, MD**
Departments of Radiology (C.M.K., K.H., J.M.D., F.H.E.), Medicine (Cardiovascular Division) (C.M.K.), Surgery (Thoracic and Cardiovascular) (J.A.K.), and Pathology (L.A.C.), University of Virginia Health System, Charlottesville, Va

Abstract

Background—MRI can distinguish components of atherosclerotic plaque. We hypothesized that contrast enhancement with gadolinium-DTPA (Gd-DTPA) could aid in the differentiation of plaque components in abdominal aortic aneurysm (AAA).

Methods and Results—Twenty-three patients (19 males, age 70±8 years) with AAA underwent MRI on a 1.5-T clinical scanner 3±3 days before surgical grafting. T1- and T2-weighted (W) black blood spin echo imaging was performed in 1 axial slice, and the T1-W imaging was repeated after a Gd-DTPA–enhanced 3D magnetic resonance angiogram. A section of the aorta at the site of imaging was resected at surgery for histopathologic examination of tissue components and inflammatory cells. Signal-to-noise and contrast-to-noise ratios (CNR) were measured in visualized plaque components from multispectral MRI, and percent enhancement after contrast on T1-W imaging was calculated. The κ value for agreement between pathology and MRI for the number of tissue components was 0.785. T2-W imaging identified thrombus as regions of high signal and lipid core as low signal, with a CNR of 6.43±3.41. Nine patients had a fibrous cap pathologically, which was visualized as a discrete area of uniform increased signal on T2-W imaging with a CNR of 4.52±1.93 compared with lipid core. Within the cap, the percent enhancement after Gd-DTPA on T1-W imaging was 91±63%.

Conclusions—Higher signal on T2-W MRI identifies the fibrous cap and thrombus within AAA. Contrast enhancement improves delineation of the fibrous cap. The addition of contrast to MRI plaque imaging may enhance identification of vulnerable plaque.

Keywords

magnetic resonance imaging; atherosclerosis; contrast media; inflammation; plaque

Atherosclerotic plaque stability depends on 3 factors: (1) the extent of the lipid core, (2) the fibrous cap and its thickness, and (3) inflammation within the cap.[1] The vulnerable plaque is considered to have a thin or ruptured fibrous cap, large lipid core, and significant inflammatory cell infiltration.[1–3] MRI has recently shown potential for the noninvasive evaluation of plaque size[4] and constituents[5–9] such as the fibrous cap, lipid core, calcified plaque, and intimal-medial hyperplasia, as well as plaque rupture.[10] The effect of therapies, such as lipid lowering, on these components has begun to be studied.[11] The ultimate goal of noninvasive imaging is to be able to discriminate these components in vivo in the coronary and carotid arteries. Image

Correspondence to Christopher M. Kramer, MD, University of Virginia Health System, Departments of Medicine and Radiology, Lee Street, Box 800170, Charlottesville, VA 22908. ckramer@virginia.edu.

resolution is such that developmental work has been performed in larger arteries such as the carotids and aorta.

Differentiation of fibrous cap from other tissues and detection of inflammation within plaque is an important goal. Contrast agents offer potential benefits in this regard. Contrast enhancement with gadolinium-DTPA (Gd-DTPA) has been demonstrated to be equivalent to or better than T2-weighted (W) imaging for discriminating fibrous cap from lipid core in a small group of patients with carotid disease.[12] Another study suggests that circulating markers of inflammation correlate with magnetic resonance (MR) markers of atherosclerosis, which include the extent of Gd-DTPA enhancement of the plaque.[13] Neovascularization within atherosclerotic plaque has also been identified after contrast.[14] We hypothesized that MRI could identify components of atherosclerotic plaque in patients with an abdominal aortic aneurysm (AAA) and that MRI techniques that include contrast enhancement could identify the fibrous cap and detect inflammation within the cap as validated by histopathology.

Methods

Patients undergoing open grafting of AAAs were recruited into the study before surgery. Patients who were scheduled for endograft repair of their AAA were excluded because no tissue would be available for comparison. All patients signed informed consent forms, and the study protocol was approved by the Human Investigation Committee of the University of Virginia.

Imaging was performed on a Siemens Vision 1.5-T MR scanner with a 4-element phased-array coil around the abdomen. ECG monitoring and gating was performed. After scout imaging, a multislice T2-W turbo spin echo sequence was performed to define a transverse plane demonstrating significant plaque burden within the aneurysm. Subsequently, T1-W images were acquired in that plane with a cardiac-gated, breath-hold, segmented, turbo spin echo sequence with repetition time (TR) of 1×RR interval, echo time (TE) of 32 ms, echo train length (ETL) of 9, and 180° refocusing radiofrequency pulses. T2-W images were obtained in the same plane by a similar turbo spin echo sequence but with a longer TE (80 ms), a longer TR (2×RR interval), and an ETL of 23 (Figure 1, top left). All sequences contained a dark blood preparation pulse (selective 180°/nonselective 180°) to reduce artifacts from blood[15,16] and were performed in single breath-hold acquisitions. Field of view (FOV) was 320 mm and matrix 264×512, which yielded a pixel size of 1.21×0.62 mm^2 with 7-mm slice thickness.

A 3D Gd-DTPA–enhanced MR angiogram of the aneurysm (TR 4 ms, TE 1.6 ms, slab thickness 96 mm with 48 partitions, 30° flip angle, 360 mm FOV, 160×256 matrix, and 2 acquisitions) was then performed during infusion of 0.1 mmol/kg Gd-DTPA (Magnevist, gadopentetate dimeglumine; Figure 2). The T1-W imaging was repeated ≈5 minutes after Gd-DTPA infusion with identical parameters as before contrast (Figure 1, top right).

The surgeon was shown the site of MRI relative to landmarks (eg, renal arteries) in order to localize the region of the aneurysm to resect (Figure 2). During surgery, the aneurysm was opened longitudinally. A 1-cm-thick cross section of the aorta at the landmarked location was resected for histopathologic examination. Approximately 10% of the posterior wall of the aneurysm was left intact for ease of closure. The surgeon marked the anterior surface of the resected circumference of the aneurysm with a suture.

Each specimen was suspended on a whole tissue mount and photographed. The tissue was blocked in by the pathologist, who examined hematoxylin-and-eosin–stained sections that were 4 μm thick. The pathologist blinded to the MRI findings histologically assessed the plaques for the presence of a fibrous cap, inflammatory cells in the fibrous cap and body of the plaque, number of layers of thrombus and plaque components, and extent of lipid (Figure 1, bottom

panels). Extent of inflammatory cell infiltration in the fibrous cap was assessed as the average number of white blood cells (WBC) per high-powered field (hpf).

An investigator (JMD) blinded to the pathological findings analyzed the number of visualized layers within the plaque by MRI, initially on T2-W imaging. All images were analyzed with Image J software (National Institutes of Health). Signal intensity was averaged from 3 circular regions of interest (ranging from 1 to 2 mm in diameter) within each visualized plaque component on the T2-W MRI that were then copied on each of 2 additional images (T1-W, post–Gd-DTPA T1-W) at equivalent locations. Noise was measured on each image, and signal-to-noise ratio (SNR) for each plaque component was calculated. The contrast-to-noise ratio (CNR) between visualized plaque constituents within plaque on T1 and T2-W imaging was measured. Percent enhancement for all visualized plaque components from pre–Gd-DTPA to post–Gd-DTPA on T1-W imaging was measured. Thickness of the fibrous cap was measured at 5 evenly spaced locations around the cap and averaged. Another investigator (CMK) compared the MRI findings directly to pathology to ensure proper matching of the images to the pathological specimens.

Cohen's κ test was used to test the agreement between pathology and MRI for the number of tissue component layers visualized. Results for SNR and CNR of tissue components between imaging sequences were analyzed by ANOVA. Precontrast to postcontrast signal enhancement was analyzed by a 2-tailed Student's paired *t* test. SNR and percent enhancement between caps with and without inflammation were compared by 2-tailed unpaired *t* test.

Results

Twenty-three patients (19 males) with a mean±SD age of 70±8 years were recruited before scheduled surgery for elective repair of AAA. The greatest diameter of the aneurysms measured by ultrasound or computed tomography before scheduling of the surgery was on average 5.9 ±0.8 cm. Patients underwent MRI at a mean of 3±3 days before the operative procedure.

Pathology demonstrated that patients had between 1 and 3 layers of plaque constituents across the plaque surface (Table 1). These components included the fibrous cap, thrombus, and/or a lipid rich core. In 5 patients, fibrous cap, thrombus, and lipid core were identified (Figure 1, top left). Two others had fibrous cap and thrombus, and another 2 had a fibrous cap and lipid core identified. The most common finding was no cap with both thrombus and lipid core seen (n=12; Figure 3), and another 2 patients had homogenous thrombus only.

The κ value for agreement between pathology and MRI for the number of components visualized was 0.785 (21 of 23 specimens were concordant; Table 1). MRI did not identify an unambiguous fibrous cap in 1 patient primarily because of suboptimal image quality but also because of significant residual contrast in the blood pool on post–Gd-DTPA imaging in that patient. In another patient, areas of both high and low signal on T2-W imaging were seen within the plaque underlying a cap, consistent with both thrombus and lipid core. However, the cap and lipid core, but no thrombus, were noted by pathological examination. This may have been because the pathological specimen was less circumferential in this patient and could have sampled only the region of lipid core.

MRI identified thrombus as regions of high signal on T2-W imaging (SNR 13.44±3.80) and lipid core as lower signal (SNR 6.75±2.85; Figures 1 [top left] and 3; Table 2). The CNR for thrombus to lipid core on T2-W imaging was 6.43±3.14. On T1-W imaging, the SNR was 15.61±7.42 for thrombus and 12.19±6.40 for lipid (Figure 4). The CNR for thrombus to lipid was 3.41±4.06 and did not increase significantly after contrast (Table 2). Percent enhancement on T1-W imaging was 4±18% (*P*=NS) for thrombus and 12±31% (*P*=NS) for lipid core. Nine

patients had regions of significant calcification within plaque. This was identified in 7 of the 9 patients as a region of signal loss consistent across all imaging sequences.

By histopathology, there was a clearly demarcated fibrous cap in 9 of the aortic samples in the 23 patients. The fibrous cap was visualized by MRI as a discrete area of uniform increased signal on T2-W imaging that ran along the luminal surface of the entire plaque circumferentially. In 1 case, the cap was thick, measuring 7.1 mm, but in all others, this was visualized as a thin layer measuring 1.7±0.4 mm thick (range 1.4 to 2.4 mm). This layer demonstrated higher signal intensity on average than that of lipid core on T2-W imaging, with a mean CNR of 4.52±1.93 (Figure 1, top left) and was less well discriminated on T1-W imaging (CNR of 2.82±3.77). However, the cap demonstrated an increase in signal on T1-W imaging after the infusion of Gd-DTPA. Percent enhancement from pre–Gd-DTPA to post–Gd-DTPA was 91±63% for T1-W imaging ($P<0.02$), and CNR for cap compared with lipid was 7.78±3.88 on contrast-enhanced T1-W imaging ($P<0.05$ versus T2-W and T1-W imaging; Figures 1 [top right] and 4).

Of the 9 patients with a fibrous cap demonstrated histologically, 5 had evidence of inflammatory cellular infiltrate within the cap, with between 15 and 120 WBC/hpf (Figure 1), and 4 did not. Four of the 5 with inflammation had a clearly visible fibrous cap by MRI. SNR for caps with and without inflammation for T2-W and T1-W imaging are shown in Table 3. The CNR compared with lipid core for T2-W imaging was 4.86±2.63 in those with inflammation and 4.10±0.56 in those without (P=NS). However, there tended to be a greater increase in postcontrast enhancement on T1-W imaging in patients with infiltration of inflammatory cells identified within the fibrous cap (123±67%) compared with those without inflammation (51±29%, $P<0.08$; Table 3).

Discussion

The present study demonstrates that MRI can noninvasively demonstrate the components of atherosclerotic plaque within AAA. The presence of a fibrous cap, thrombus, and lipid core can be identified with very good agreement with histopathology. T2-W imaging is quite useful for differentiating plaque components and was used to make the initial differentiation of thrombus and lipid components. Higher signal on T2-W MRI helps to identify both the fibrous cap and thrombus. Contrast enhancement with Gd-DTPA improves delineation of the fibrous cap on T1-W imaging. Contrast enhancement within the fibrous cap may add to the evaluation of the vulnerable plaque.

MRI has been shown to correlate well with transesophageal echocardiography for delineation of the size and extent of plaque in the descending aorta.[17] Plaque regression with lipid-lowering therapy can likewise be quantified in both the aorta and carotids.[18] Transesophageal MRI with a loopless radiofrequency receiver inside a nasogastric tube has been shown to more accurately measure the thickness and circumferential extent of aortic plaque compared with transesophageal echocardiography.[19] To the best of our knowledge, the present study is the first to examine aortic plaque morphology in humans and to compare it to histopathology.

The utility of MR for differentiation of plaque components has been increasingly recognized. Investigators first demonstrated that water T2 is shorter in the lipid-rich core of atherosclerotic plaques than in the collagenous cap or normal media.[20] Later, the same group used T2-W imaging to identify fibrocellular, calcified, lipid, and thrombotic components.[6] Shinnar et al[7] demonstrated high accuracy of ex vivo MRI in carotid endarterectomy specimens and proposed MRI criteria for differentiating calcium, fibrocellular, lipid core, and thrombus components. Later in vivo studies in animals confirmed these findings, demonstrating the ability of MRI to differentiate plaque components in vivo.[21] More recent studies in humans corroborate this

ability to define plaque morphology with multispectral MRI in carotid arteries[8] and have shown good correlation with American Heart Association–defined classification of plaque.[9] The present study confirms this capability in aortic atherosclerosis.

Thrombus can be identified in vivo,[22] but its signal characteristics on T2-W imaging may depend on its age, because higher signal is seen on thrombus up to 1 week in age, which declines thereafter.[23] Exact identification of the age of thrombus was not possible in the present study.

Investigators have begun to examine the relationship between contrast enhancement and atherothrombosis as evaluated by MRI. Enhancement after infusion of contrast agents has been examined in balloon-injured carotid arteries.[24]The vessel walls were visualized by MR angiography even in the presence of thrombotic occlusion, and this was thought to be due to neovascularization in the neointima or the thrombus. Another study also suggested that neovascularization accounts for contrast uptake in atherosclerotic plaque.[25] These investigators demonstrated that fibrous tissue showed a mean increase in signal intensity after contrast of 79.5% for fibrous tissue and less for the necrotic core (28.6%). They found regions of neovascularization within a subset of fibrous regions that accounted for much of the increase in signal intensity. No neovascularization was seen by histopathology in the present study, although special stains to identify neovascularization were not used. In another study of 84 patients with carotid atherosclerosis, carotid walls showed hypointense inner rims and enhancement of the outer rim after Gd-DTPA infusion.[26] The investigators hypothesized that this enhancement was due to angiogenesis within the wall, although no histopathologic confirmation was available.

A recent study correlated serum markers of inflammation in humans with MR markers of plaque in the aorta and common carotids.[13] MR markers of plaque included increased wall thickness, higher T2-W signal intensity, and increased contrast enhancement values after Gd-DTPA infusion.[13] These patients with MRI markers of plaque had higher values of interleukin-6, C-reactive protein, vascular cell adhesion molecule-1, and intercellular adhesion molecule-1 than those without MRI markers, which suggests the association of MRI findings, including contrast enhancement, with inflammation.

The present study is consistent with the finding of prior investigations that enhancement of the fibrous cap after Gd-DTPA improves its delineation, increasing the SNR of fibrous cap and lipid core without loss of CNR between these components.[12] The increase in signal seen in the study by Wasserman et al[12] was 28.7% for short TR images, less than that seen in the present study. The absolute thickness of the cap is much less in the carotid (usually <0.25 mm) than in AAA (on average 1.7 mm in the present study), and the extent of contrast uptake may be more difficult to discern even though image resolution is superior in carotid imaging. This may have important implications for coronary plaque imaging in which the fibrous cap is on the order of 65 to 150 μm thick.[3]

Study Limitations

Atherosclerotic plaque in AAA may be quite different from that in carotid or coronary arteries. For one, the extent of thrombus is greater. However, MR techniques are able to differentiate tissue components regardless of the nature of the composition of plaque in different arterial systems. The nature of inflammation in the fibrous cap in the present study was primarily acute. This may be different from the monocyte/macrophage predominance in carotid and coronary plaque, and the findings of increased Gd-DTPA uptake in the cap may not be extrapolated to these locations. Because a fibrous cap was not a uniform finding in AAA in the present study (9 of 23 patients), the power of the study to detect differences in signal intensity as a marker of inflammation within the cap was lower than anticipated. Matching of inflammation and

contrast enhancement on a segmental basis along the circumference of the plaque was not performed.

Misregistration error could have occurred if the surgeon resected an area of the AAA different from that imaged. However, care was taken to landmark the site imaged relative to the renal arteries to enable the surgeon to identify the region to resect. Proton-density–weighted imaging was not used in the present study because a review of the literature demonstrates that T2-W and T1-W imaging are more useful for discriminating tissue components.[7–9,21] The time after contrast for T1-W imaging was slightly variable owing to time-consuming reconstruction of the MR angiogram, which may introduce variability into the postcontrast signal-intensity measurements.

Some of the postcontrast T1-W images demonstrated unsuppressed contrast (Figure 1). A quadruple inversion recovery sequence may have reduced this problem.[27]

Acknowledgments

This study was supported by a grant from the Commonwealth of Virginia Health Research Board. We acknowledge John Oshinski, PhD, for his help in study planning and initial sequence design, Jennifer Hunter, RN, for her patient recruitment efforts, and John Christopher, RT, for his imaging expertise.

References

1. Falk E. Why do plaques rupture? Circulation 1992;86(suppl III):III-30–III-42. [PubMed: 1424049]
2. Ross R. Atherosclerosis: an inflammatory disease. N Engl J Med 1999;340:115–126. [PubMed: 9887164]
3. Fayad ZA, Fuster V. Clinical imaging of the high-risk or vulnerable atherosclerotic plaque. Circ Res 2001;89:305–316. [PubMed: 11509446]
4. Yuan C, Beach KW, Smith LH Jr, et al. Measurement of atherosclerotic carotid plaque size in vivo using high resolution magnetic resonance imaging. Circulation 1998;98:2666–2671. [PubMed: 9851951]
5. Skinner MP, Yuan C, Mitsumori L, et al. Serial magnetic resonance imaging of experimental atherosclerosis detects lesion fine structure, progression and complications in vivo. Nat Med 1995;1:69–73. [PubMed: 7584956]
6. Toussaint JF, LaMuraglia GM, Southern JF, et al. Magnetic resonance images lipid, fibrous, calcified, hemorrhagic, and thrombotic components of human atherosclerosis in vivo. Circulation 1996;94:932–938. [PubMed: 8790028]
7. Shinnar M, Fallon JT, Wehrli S, et al. The diagnostic accuracy of ex vivo MRI for human atherosclerotic plaque characterization. Arterioscler Thromb Vasc Biol 1999;19:2756–2761. [PubMed: 10559022]
8. Yuan C, Mitsumori LM, Ferguson MS, et al. In vivo accuracy of multispectral magnetic resonance imaging for identifying lipid-rich necrotic cores and intraplaque hemorrhage in advanced human carotid plaques. Circulation 2001;104:2051–2056. [PubMed: 11673345]
9. Cai JM, Hatsukami TS, Ferguson MS, et al. Classification of human carotid atherosclerotic lesions with in vivo multicontrast magnetic resonance imaging. Circulation 2002;106:1368–1373. [PubMed: 12221054]
10. Yuan C, Zhang SX, Polissar NL, et al. Identification of fibrous cap rupture with magnetic resonance imaging is highly associated with recent transient ischemic attack or stroke. Circulation 2002;105:181–185. [PubMed: 11790698]
11. Zhao XQ, Yuan C, Hatsukami TS, et al. Effects of prolonged intensive lipid-lowering therapy on the characteristics of carotid atherosclerotic plaques in vivo by MRI: a case-control study. Arterioscler Thromb Vasc Biol 2001;21:1623–1629. [PubMed: 11597936]
12. Wasserman BA, Smith WI, Trout HH, et al. Carotid artery atherosclerosis: in vivo morphologic characterization with gadolinium-enhanced double-oblique MR imaging: initial results. Radiology 2002;223:566–573. [PubMed: 11997569]

13. Weiss CR, Arai AE, Bui MN, et al. Arterial wall MRI characteristics are associated with elevated serum markers of inflammation in humans. J Magn Reson Imaging 2002;2001:698–704.

14. Kerwin W, Hooker A, Spilker M, et al. Quantitative magnetic resonance imaging analysis of neovasculature volume in carotid atherosclerotic plaque. Circulation 2003;107:851–856. [PubMed: 12591755]

15. Edelman RR, Chien D, Kim D. Fast selective black blood MR imaging. Radiology 1991;181:655–660. [PubMed: 1947077]

16. Simonetti OP, Finn JP, White RD, et al. "Black blood" T2-weighted inversion-recovery MR imaging of the heart. Radiology 1996;199:49–57. [PubMed: 8633172]

17. Fayad ZA, Nahar T, Fallon JT, et al. In vivo magnetic resonance evaluation of atherosclerotic plaques in the human thoracic aorta: a comparison with transesophageal echocardiography. Circulation 2000;101:2503–2509. [PubMed: 10831525]

18. Corti R, Fayad ZA, Fuster V, et al. Effects of lipid-lowering by simvastatin on human atherosclerotic lesions: a longitudinal study by high-resolution, noninvasive magnetic resonance imaging. Circulation 2001;104:249–252. [PubMed: 11457739]

19. Shunk KA, Garot J, Atalar E, et al. Transesophageal magnetic resonance imaging of the aortic arch and descending thoracic aorta in patients with aortic atherosclerosis. J Am Coll Cardiol 2001;37:2031–2035. [PubMed: 11419883]

20. Toussaint JF, Southern JF, Fuster V, et al. T2-weighted contrast for NMR characterization of human atherosclerosis. Arterioscler Thromb Vasc Biol 1995;15:1533–1542. [PubMed: 7583524]

21. Worthley SG, Helft G, Fuster V, et al. High resolution ex vivo magnetic resonance imaging of in situ coronary and aortic atherosclerotic plaque in a porcine model. Atherosclerosis 2000;150:321–329. [PubMed: 10856524]

22. Johnstone MT, Botnar RM, Perez AS, et al. In vivo magnetic resonance imaging of experimental thrombosis in a rabbit model. Arterioscler Thromb Vasc Biol 2001;21:1556–1560. [PubMed: 11557688]

23. Corti R, Osende JI, Fayad ZA, et al. In vivo noninvasive detection and age definition of arterial thrombus by MRI. J Am Coll Cardiol 2002;39:1366–1373. [PubMed: 11955857]

24. Lin W, Abendschein DR, Haacke EM. Contrast-enhanced magnetic resonance angiography of carotid arterial wall in pigs. J Magn Reson Imaging 1997;7:183–190. [PubMed: 9039613]

25. Yuan C, Kerwin WS, Ferguson MS, et al. Contrast-enhanced high resolution MRI for atherosclerotic carotid artery tissue characterization. J Magn Reson Imaging 2002;15:62–67. [PubMed: 11793458]

26. Aoki S, Aoki K, Ohsawa S, et al. Dynamic MR imaging of the carotid wall. J Magn Reson Imaging 1999;9:420–427. [PubMed: 10194712]

27. Yarnykh VL, Yuan C. T1-insensitive flow suppression using quadruple inversion-recovery. Magn Reson Med 2002;48:899–905. [PubMed: 12418006]

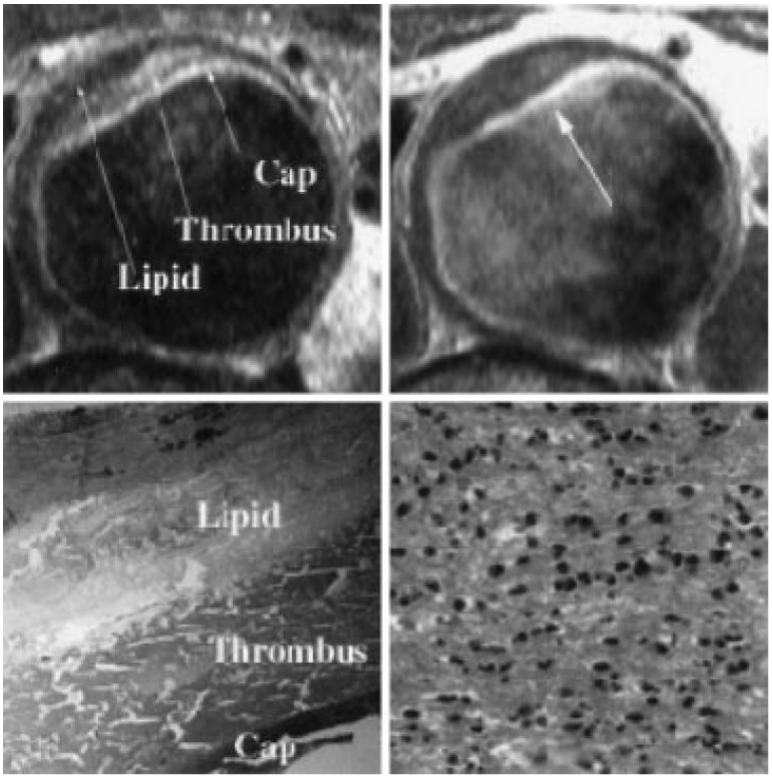

Figure 1.
Top left, T2-weighted MRI of AAA with 3 components visualized within plaque as marked. Top right, T1-weighted MRI after Gd-DTPA infusion with very high signal intensity seen in luminal layer, which was identified as fibrous cap by histopathology. Percent enhancement relative to pre–Gd-DTPA T1-W image was 143%. Bottom left, Histopathology showing fibrous cap, thrombus, and lipid corresponding to components visualized by MRI. Bottom right, High power of fibrous cap demonstrating dense infiltration of polymorphonuclear leukocytes (120 WBC/hpf).

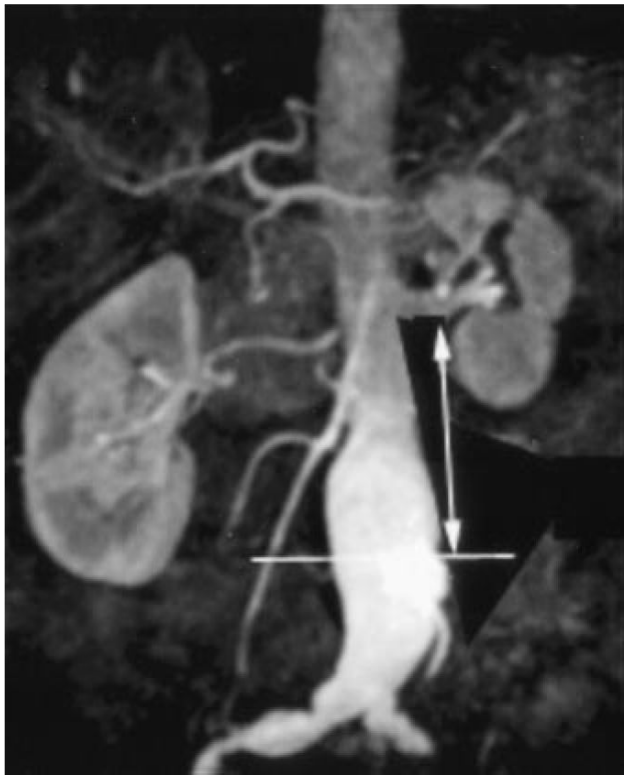

Figure 2.
3D MR angiogram with Gd-DTPA enhancement with horizontal line demonstrating location of area imaged with multi-spectral MRI within AAA. Landmarked distance from left renal artery is shown with double-headed arrow. This was shown to surgeon to mark site for resection at time of AAA grafting.

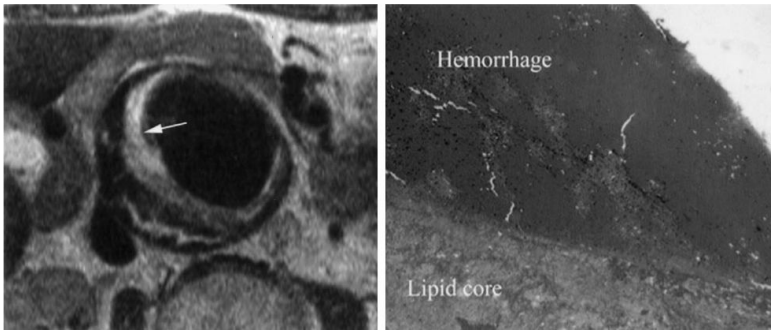

Figure 3.
On left is T2-W turbo spin echo image with double-inversion pulse demonstrating plaque within AAA. Very bright signal along luminal surface of plaque on left (identified by arrow) is acute hemorrhage as demonstrated on correlative histopathologic specimen on right. Deep to acute hemorrhage is tissue with low signal intensity on T2-W imaging consistent with lipid core as validated on pathology. No fibrous cap was seen either on MRI or pathological examination.

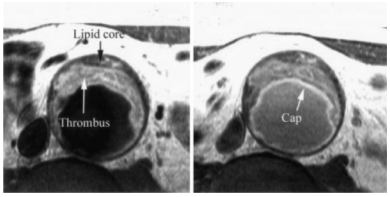

Figure 4.

Left, T1-W turbo spin echo image in patient with AAA demonstrating bright signal within thrombus and darker signal in lipid core toward vessel wall. Cap is faintly seen on T1-W imaging. Right, T1-W image as above but several minutes after infusion of Gd-DTPA. Note improved delineation of fibrous cap by bright signal within (arrow).

TABLE 1

Clinical and Pathological Data on Study Patients

Patient	Age, y	AAA Size, cm	Components by Pathology	Components by MRI	Fibrous Cap by Histology	Inflammation in Cap by Histology
1	70	7.0	3	3	+	+
2	70	6.7	3	3	−	…
3	80	5.5	1	1	−	…
4	73	6.0	2	2	−	…
5	64	6.0	3	2	+	+
6	68	5.0	2	2	−	…
7	82	8.0	2	2	+	−
8	72	6.8	2	2	−	…
9	78	6.5	2	2	+	−
10	56	5.0	2	2	+	−
11	71	5.5	2	2	+	+
12	68	5.6	2	2	−	…
13	70	7.0	2	2	−	…
14	63	4.8	2	2	−	…
15	72	4.8	2	2	−	…
16	53	5.0	2	2	+	+
17	63	5.5	3	3	−	…
18	74	5.4	2	2	+	+
19	69	5.3	3	3	−	…
20	63	5.6	2	2	−	…
21	68	6.0	2	2	−	…
22	66	5.5	2	3	+	−
23	86	7.0	2	2	−	…

TABLE 2

SNR and CNR for Plaque Components on T2-W and T1-W Imaging

	T2-W Imaging	T1-W Imaging	T1-W Imaging After Contrast	ANOVA *P*
SNR fibrous cap	11.47±3.79	12.69±6.61	19.90±9.42	<0.10
SNR thrombus	13.44±3.80	15.61 ±7.42	17.58±10.49	NS
SNR lipid core	6.75±2.85	12.19±6.40*	12.50±7.62*	<0.01
CNR fibrous cap/lipid	4.52±1.93	2.82±3.77	7.78±3.88**	<0.01
CNR thrombus/lipid	6.43±3.41	3.41 ±4.06	5.08±6.00	0.09

*P<0.05 vs T2-W imaging.

†P<0.05 vs T1-W imaging.

TABLE 3

SNRs for Fibrous Caps With and Without Inflammation on T2-W and T1-W Imaging and Percent Enhancement on T1-W Imaging After Gd-DTPA

	T2-W Imaging (SNR)	T1-W Imaging (SNR)	% Enhancement After Gd-DTPA
Cap with inflammation	12.39±4.96	12.2±11.93	123±67%
Cap without inflammation	10.33±1.54	13.63±6.97	51±29%
P	NS	NS	<0.08